

# DYNAMIC ANALYSIS OF FG STEPPED TRUNCATED CONICAL SHELLS SURROUNDED BY PASTERNAK ELASTIC FOUNDATIONS

Le Quang Vinh<sup>1,\*</sup>, Nguyen Manh Cuong<sup>2</sup>

<sup>1</sup>*Viet Tri University of Industry, Phu Tho, Vietnam*

<sup>2</sup>*Hanoi University of Science and Technology, Vietnam*

E-mail: [vinhchc@gmail.com](mailto:vinhchc@gmail.com)

Received: 28 December 2019 / Published online: 28 June 2020

**Abstract.** This research presents a continuous element model for solving vibration problems of FG stepped truncated conical shells having various material properties and surrounded by Pasternak foundations. Based on the First Order Shear Deformation Theory (FSDT) and the equations of the FGM conical shells, the dynamic stiffness matrix is obtained for each segment of the shell having constant thickness. The interesting assembly procedure of continuous element method (CEM) is employed for joining those segments in order to analyze the dynamic behavior of the FG stepped truncated conical shells an assembly procedure of continuous element method (CEM) is employed for joining those segments. Free vibrations of different configurations of FG stepped truncated conical shells on elastic foundations are examined. Effects of structural parameters, stepped thickness and elastic foundations on the free vibration of FG stepped truncated conical shells are also presented.

*Keywords:* stepped shell, vibration of conical shell, functionally graded shell, continuous element method, Winkler–Pasternak foundation.

## 1. INTRODUCTION

Conical shells are widely used in modern engineering structures such as tunnels, storage tanks, pressure vessels, rockets, missiles, water ducts, pipelines and casing pipes and in other applications. Therefore, static and dynamic analysis of shells in interaction with elastic media is important for the safety and stability of those structures. Most earthen soils can appropriately be represented by the Pasternak model, whereas sandy soils and liquids can be represented by Winkler's model [1, 2]. The static and dynamic analyses of conical shells on elastic foundations have been studied in recent years. For FGM conical shells resting on elastic foundations, many significant results on the vibration and dynamic buckling of FGM conical shells are obtained. Sofiyev and Kuruoglu [3]

studied vibrations of FGM truncated and complete conical shells resting on elastic foundations under various boundary conditions by applying the Galerkin method. The considered elastic foundations include the Winkler- and Pasternak-type elastic foundations. The FGMs are assumed to vary as power and exponential functions through the thickness of the conical shells. Sofiyev and Schnack [4] presented solutions for the vibration analysis of truncated conical shells made of FGM and resting on the Winkler–Pasternak foundations. The governing equations according to the Donnell’s theory are solved by Galerkin’s method and the fundamental frequencies with or without two-parameter elastic foundation have been investigated. Dung et al. [5] presented an analytical approach to investigate the mechanical buckling load of eccentrically stiffened functionally graded truncated conical shells surrounded by elastic medium and subjected to axial compressive load and external uniform pressure based on the classical shell theory and Galerkin method.

The stepped conical shells (SCSs) structures offer challenging vibration problems not only due to the degree of complexity of the governing shell equations, but also due to the difficulty associated with matching the continuity conditions between the shell components. Although finite element computer codes (NASTRAN, ANSYS, ABAQUS, etc.) can analyze the vibrations of these SCSs and have been well developed and managed, the disadvantage is that the computation cost is quite expensive. Xie et al. [6] presented a unified approach to determine natural frequencies and forced vibration responses of stepped conical shells with arbitrary boundary conditions. The approach is involved in dividing the stepped shells into narrow segments at the locations of discontinuities of thickness and semi-vertex angle. Flügge theory is used to describe equations of motions of conical segments and displacement functions are expanded as power series. Qu et al. [7] developed an efficient domain decomposition algorithm for free and forced vibration analysis of the uniform and stepped conical shells subjected to classical and nonclassical boundary conditions. Vinh et al. [8] present a new Continuous Element for analyzing dynamic behavior of stepped composite conical shells. In this work, a powerful assembly procedure has been presented for constructing new dynamic stiffness matrix of stepped composite conical shells. The continuous element formulations here are established based on the analytical solution of differential equations for composite conical shells giving high precision results. Nam et al. [9] presented a continuous element model for solving vibration problems of stepped composite cylindrical shells surrounded by Pasternak foundations with various boundary conditions. Based on the First Order Shear Deformation Theory (FSDT), the equations of motion of the circular cylindrical shell are introduced and the dynamic stiffness matrix is obtained for each segment of the uniform shell. The assembly procedure of continuous element method (CEM) is adopted to analyze the dynamic behavior of the stepped composite cylindrical shell surrounded by an elastic foundation. Available vibration study results in the literature for SCSs are few and far between, as it has not received much attention of the researchers, perhaps due to the complexity involving in the modeling and solution procedure. Therefore, a unified method which can be both accurate and efficient to determine the natural frequencies and forced vibration responses of the SCSs would be highly desirable.

The main purpose of this paper is to present a new Continuous Element model to analyze the dynamic behavior of the multi FG stepped truncated conical shells with various material characteristics and surrounded by Winkler-Pasternak foundations. Based on the assembly procedure of single continuous elements, the dynamic stiffness matrix of complex stepped conical shells surrounded by Pasternak foundation is established. In this research, the influences of different parameters are studied in detail such as: stepped thickness, geometrical ratios and elastic foundation stiffness. The achieved numerical results are compared to those calculated by the finite element method and by other researches in some singular cases. The efficiency and accuracy as well as the saving in data storage and computed time of the CE method for complex shells in contact with elastic foundations in medium and high frequencies have been investigated and confirmed in this study.

## 2. THEORETICAL FORMULATION

### 2.1. Description of the model

Let's investigate the FGM conical shell with  $(x, \theta, z)$  coordinates, as shown in Fig. 1. The coordinate  $x$  is measured along the cone generator with the origin placed at the middle of the generators;  $\theta$  is the circumferential coordinate and  $z$  is the perpendicular to the shell surfaces.  $R_1$  and  $R_2$  are the small and large radii of cone cross sections, respectively (see Fig. 1);  $h$  is the thickness, the cone length and cone semi-vertex angle of the shell are represented by  $L$  and  $\alpha$  and the radius coordinate  $R(x)$  of a point  $M$  inside the shell is calculated as:  $R(x) = R_1 + x \sin \alpha$ .

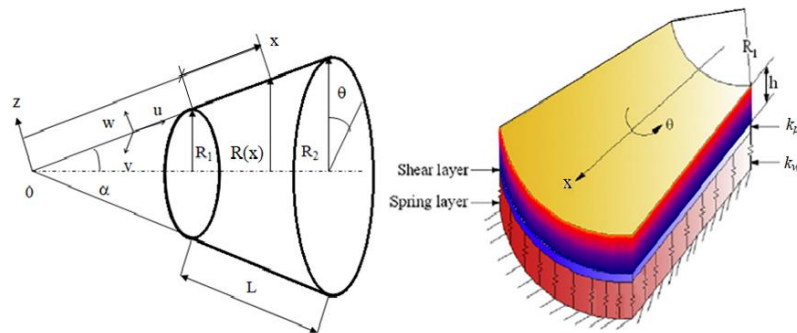


Fig. 1. Geometry parameters of a FG truncated conical shell surrounded by Pasternak elastic foundation

This shell is surrounded by a Winkler elastic foundation having a foundation stiffness  $k_w$  or by a Pasternak foundation with the foundation stiffness  $k_w$  and shear layer stiffness  $k_p$ . Such shell is the basic continuous shell element to contribute a FG truncated conical shell surrounded by two above types of elastic foundations.

Typically, FGM shells are made from a mixture of two material phases. In this paper, it is assumed that the FGM shells are made of a mixture of ceramic and metal. Young's modulus  $E(z)$ , density  $\rho(z)$  and Poisson's ratio  $\mu(z)$  are assumed to vary continuously

through the shell thickness and can be expressed as a linear combination

$$\begin{aligned} E(z) &= (E_c - E_m)V_c + E_m, \\ \mu(z) &= (\mu_c - \mu_m)V_c + \mu_m, \\ \rho(z) &= (\rho_c - \rho_m)V_c + \rho_m, \end{aligned} \quad (1)$$

where the subscripts  $c$  and  $m$  represent the ceramic and metallic constituents, respectively, and the volume fraction  $V_c$  follows two general four-parameter power-law distributions [3,6,8]

$$\begin{aligned} FGM_{I(a/b/c/p)} : V_c &= \left[ 1 - a \left( \frac{1}{2} + \frac{z}{h} \right) + b \left( \frac{1}{2} + \frac{z}{h} \right)^c \right]^p, \\ FGM_{II(a/b/c/p)} : V_c &= \left[ 1 - a \left( \frac{1}{2} - \frac{z}{h} \right) + b \left( \frac{1}{2} - \frac{z}{h} \right)^c \right]^p, \end{aligned} \quad (2)$$

in which the power-law exponent  $p$  is a positive real number ( $0 \leq p \leq \infty$ ) and the parameters  $a, b, c$  represent the material variation profile through the functionally graded shell thickness. It is assumed that the sum of the volume fractions of the two basic components is equal to unity, i.e.,  $V_c + V_m = 1$ . Therefore, according to the relations defined in Eq. (2), when the power-law exponent  $p$  is set equal to zero (i.e.,  $p = 0$ ) or equal to infinity (i.e.,  $p = \infty$ ), the FGM material becomes the homogeneous isotropic material, expressed as

$$\begin{aligned} p = 0 &\rightarrow V_c = 1, \quad V_m = 0 \rightarrow E(z) = E_c, \quad \mu(z) = \mu_c, \quad \rho(z) = \rho_c, \\ p = \infty &\rightarrow V_c = 0, \quad V_m = 1 \rightarrow E(z) = E_m, \quad \mu(z) = \mu_m, \quad \rho(z) = \rho_m. \end{aligned} \quad (3)$$

Whereas the composition of ceramic ( $M_1$ ) and metal ( $M_2$ ) is linear for  $p = 1$ . The variations of the volume fraction  $V_c$  through the shell thickness for different values of the power-law exponent  $p$  are illustrated in Fig. 2. In this figure, the classical volume fraction

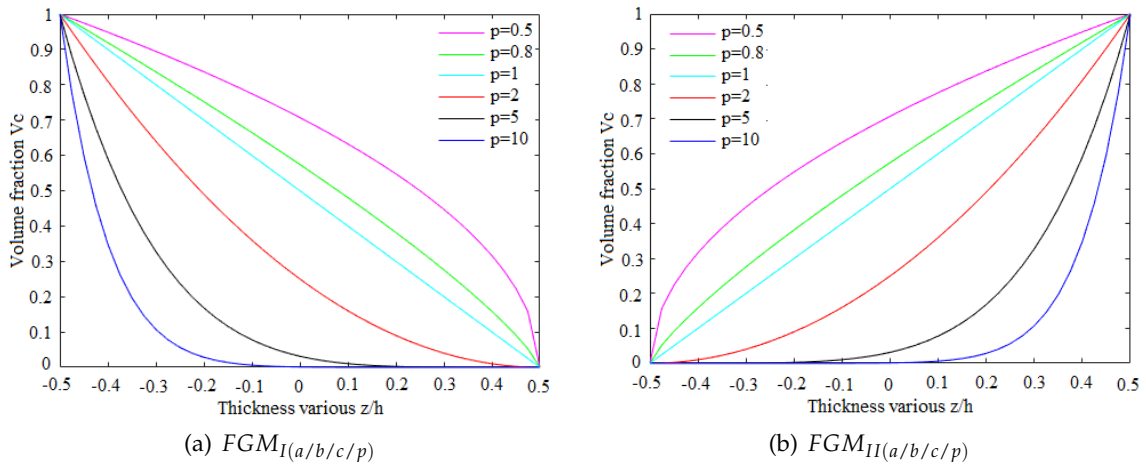


Fig. 2. Variation of the volume fraction  $V_c$  through the thickness of a shell for different values of power-law exponent  $p$

profiles, such as those reported in literature [?, ?], are presented as special cases of the general distribution laws by setting  $a = 1$  and  $b = 0$ . As can be seen from Fig. 2(a), for the first distribution FGMI ( $a = 1/b = 0/c/p$ ) the material composition is continuously varied such that the bottom surface ( $z/h = -0.5$ ) of the shell is  $M_1$  rich, whereas the top surface ( $z/h = 0.5$ ) is  $M_2$  rich. The volume fraction  $V_c$  decreased from 1 at  $z/h = -0.5$  to zero at  $z/h = 0.5$ . Fig. 2(b) shows that for the second distribution FGMII ( $a = 1/b = 0/c/p$ ) the top surface ( $z/h = 0.5$ ) of the shell is  $M_1$  rich, whereas the bottom surface ( $z/h = -0.5$ ) is  $M_2$  rich, instead. When the volume fraction exponent is increased, the content of  $M_1$  in FG layer decreases.

So far, all the needed parts of the first-order shear deformation shell theory (FSDT) are presented, and they may be combined to obtain the desired form of the equations of motion.

## 2.2. Kinematic relations and stress resultants

On the basis of the assumptions of moderately thick shell theory, the displacement components of an arbitrary point in the FG shell for the first-order shear deformation theory are expressed in terms of the displacements and rotation components of the middle surface as given below [9]

$$\begin{aligned} u(x, \theta, z, t) &= u_0(x, \theta, t) + z\varphi_x(x, \theta, t), \\ v(x, \theta, z, t) &= v_0(x, \theta, t) + z\varphi_\theta(x, \theta, t), \\ w(x, \theta, z, t) &= w_0(x, \theta, t), \end{aligned} \quad (4)$$

where  $u, v$  and  $w$  are the displacement components in the  $x, \theta$  and  $z$  directions, respectively;  $u_0, v_0$  and  $w_0$  are the middle surface displacements of the shell in the axial, circumferential and radial directions, respectively;  $\varphi_x$  and  $\varphi_\theta$  represent the transverse normal rotations of the reference surface about the  $\theta$ - and  $x$ -axis,  $t$  is the time variable. The linear strain-displacement relations in the shell space are defined as

$$\begin{aligned} \varepsilon_x &= \frac{\partial u_0}{\partial x}, & k_x &= \frac{\partial \varphi_x}{\partial x}, \\ \varepsilon_\theta &= \frac{1}{R(x)} \left( u_0 \sin \alpha + \frac{\partial v_0}{\partial \theta} + w_0 \cos \alpha \right), & k_{x\theta} &= \frac{1}{R(x)} \frac{\partial \varphi_x}{\partial \theta} + \frac{\partial \varphi_\theta}{\partial x} - \frac{\sin \alpha}{R(x)} \varphi_\theta, \\ \varepsilon_{x\theta} &= \frac{\partial v_0}{\partial x} + \frac{1}{R(x)} \frac{\partial u_0}{\partial \theta} - \frac{\sin \alpha}{R(x)} v_0, & k_\theta &= \frac{1}{R(x)} \left( \varphi_x \sin \alpha + \frac{\partial \varphi_\theta}{\partial \theta} \right), \\ \gamma_{xz} &= \frac{\partial w_0}{\partial x} + \varphi_x, & \gamma_{\theta z} &= \frac{-\cos \alpha}{R(x)} v_0 + \frac{1}{R(x)} \frac{\partial w_0}{\partial \theta} + \varphi_\theta. \end{aligned} \quad (5)$$

Based on Hooke's law, the stress-strain relations of the shell are written as

$$\begin{Bmatrix} \sigma_x \\ \sigma_\theta \\ \tau_{x\theta} \\ \tau_{xz} \\ \tau_{\theta z} \end{Bmatrix} = \begin{bmatrix} Q_{11}(z) & Q_{12}(z) & 0 & 0 & 0 \\ Q_{12}(z) & Q_{11}(z) & 0 & 0 & 0 \\ 0 & 0 & Q_{66}(z) & 0 & 0 \\ 0 & 0 & 0 & Q_{66}(z) & 0 \\ 0 & 0 & 0 & 0 & Q_{66}(z) \end{bmatrix} \begin{Bmatrix} \varepsilon_x \\ \varepsilon_\theta \\ \gamma_{x\theta} \\ \gamma_{xz} \\ \gamma_{\theta z} \end{Bmatrix}, \quad (6)$$

where the elastic constant  $Q_{ij}(z)$  are functions of thickness coordinate  $z$  and are defined as

$$Q_{11}(z) = \frac{E(z)}{1 - \mu^2(z)}, \quad Q_{12}(z) = \frac{\mu(z)E(z)}{1 - \mu^2(z)}, \quad Q_{66}(z) = \frac{E(z)}{2[1 + \mu(z)]}. \quad (7)$$

The stress and moment resultants are given as

$$(N_x, N_\theta, N_{x\theta}, Q_x, Q_\theta) = \int_{-h/2}^{h/2} (\sigma_{xx}, \sigma_{\theta\theta}, \tau_{x\theta}, \tau_{xz}, \tau_{\theta z}) dz, \quad (8)$$

$$(M_x, M_\theta, M_{x\theta}) = \int_{-h/2}^{h/2} (\sigma_{xx}, \sigma_{\theta\theta}, \tau_{x\theta}) z dz, \quad (9)$$

where  $N_x, N_\theta$  and  $N_{x\theta}$  are the in-plane force resultants,  $M_x, M_\theta$  and  $M_{x\theta}$  are moment resultants,  $Q_x, Q_\theta$  are transverse shear force resultants. The shear correction factor  $f$  is computed such that the strain energy due to transverse shear stresses in Eq. (10) are equals to the strain energy due to the true transverse stresses predicted by the three-dimensional elasticity theory [8]. In this paper, the shear correction factors  $f = 5/6$  [6, 8]. Substituting Eqs. (6)–(7) into Eqs. (8)–(9) following constitutive equations relating the force and moment resultants to strains and curvatures of the reference surface are given in the matrix form

$$\begin{Bmatrix} N_x \\ N_\theta \\ N_{x\theta} \\ M_x \\ M_\theta \\ M_{x\theta} \\ Q_x \\ Q_\theta \end{Bmatrix} = \begin{bmatrix} A_{11} & A_{12} & 0 & B_{11} & B_{12} & 0 & 0 & 0 \\ A_{12} & A_{11} & 0 & B_{12} & B_{11} & 0 & 0 & 0 \\ 0 & 0 & A_{66} & 0 & 0 & B_{66} & 0 & 0 \\ B_{11} & B_{12} & 0 & D_{11} & D_{12} & 0 & 0 & 0 \\ B_{12} & B_{11} & 0 & D_{12} & D_{11} & 0 & 0 & 0 \\ 0 & 0 & B_{66} & 0 & 0 & D_{66} & 0 & 0 \\ 0 & 0 & 0 & 0 & 0 & 0 & fF_{44} & 0 \\ 0 & 0 & 0 & 0 & 0 & 0 & 0 & fF_{55} \end{bmatrix} \begin{Bmatrix} \varepsilon_x \\ \varepsilon_\theta \\ \varepsilon_{x\theta} \\ k_x \\ k_\theta \\ k_{x\theta} \\ \gamma_{xz} \\ \gamma_{\theta z} \end{Bmatrix}. \quad (10)$$

The structure materials employed in the following study are assumed to be functionally graded and linearly elastic. So, the extensional stiffness  $A_{ij}$ , the bending stiffness  $D_{ij}$ , and the extensional-bending coupling stiffness  $B_{ij}$  are respectively expressed as

$$\begin{aligned} A_{ij} &= \int_{-h/2}^{h/2} Q_{ij}(z) dz, & B_{ij} &= \int_{-h/2}^{h/2} z Q_{ij}(z) dz, \\ D_{ij} &= \int_{-h/2}^{h/2} z^2 Q_{ij}(z) dz, \quad i, j = 1, 2, 6, & F_{ij} &= \int_{-h/2}^{h/2} Q_{ij}(z) dz, \quad i, j = 4, 5. \end{aligned} \quad (11)$$

### 2.3. Equations of motion

The equilibrium equations of motion for FG truncated conical shell surrounded by Pasternak foundation based on the first-order shear deformation shell theory (FSDT) in terms of the force and moment resultants can be written as [8]

$$\begin{aligned}
\frac{\partial N_x}{\partial x} + \frac{\sin \alpha}{R(x)}(N_x - N_\theta) + \frac{1}{R(x)} \frac{\partial N_{x\theta}}{\partial \theta} &= I_0 \ddot{u}_0 + I_1 \ddot{\varphi}_x, \\
\frac{\partial N_{x\theta}}{\partial x} + \frac{2 \sin \alpha}{R(x)} N_{x\theta} + \frac{1}{R(x)} \frac{\partial N_\theta}{\partial \theta} + \frac{\cos \alpha}{R(x)} Q_\theta &= I_0 \ddot{v}_0 + I_1 \ddot{\varphi}_\theta, \\
\frac{\partial Q_x}{\partial x} + \frac{1}{R(x)} \frac{\partial Q_\theta}{\partial \theta} + \frac{\sin \alpha}{R(x)} Q_x - \frac{\cos \alpha}{R(x)} N_\theta - k_w w + k_p \left( \frac{\partial^2 w}{\partial x^2} + \frac{\sin \alpha}{R(x)} \frac{\partial w}{\partial x} + \frac{1}{R(x)^2} \frac{\partial^2 w}{\partial \theta^2} \right) &= I_0 \ddot{w}_0, \\
\frac{\partial M_x}{\partial x} + \frac{\sin \alpha}{R(x)}(M_x - M_\theta) + \frac{1}{R(x)} \frac{\partial M_{x\theta}}{\partial \theta} - Q_x &= I_1 \ddot{u}_0 + I_2 \ddot{\varphi}_x, \\
\frac{\partial M_{x\theta}}{\partial x} + \frac{2 \sin \alpha}{R(x)} M_{x\theta} + \frac{1}{R(x)} \frac{\partial M_\theta}{\partial \theta} - Q_\theta &= I_1 \ddot{v}_0 + I_2 \ddot{\varphi}_\theta,
\end{aligned} \tag{12}$$

where

$$[I_0, I_1, I_2] = \int_{-h/2}^{h/2} \rho(z) [1, z^1, z^2] dz,$$

$\rho(z)$  is the density of the shell per unit middle surface area.  $I_0, I_1$  and  $I_2$  are the mass inertias.

### 3. DYNAMIC STIFFNESS MATRIX FORMULATION FOR FG TRUNCATED CONICAL SHELL

The chosen state-vector is  $y = u_0, v_0, w_0, \varphi_x, \varphi_\theta, N_x, N_{x\theta}, Q_x, M_x, M_{x\theta}^T$ . Next, the Fourier series expansion for state variables is written as

$$\begin{aligned}
&\{u_0(x, \theta, t), w_0(x, \theta, t), \varphi_\theta(x, \theta, t), N_x(x, \theta, t), Q_x(x, \theta, t), M_x(x, \theta, t)\}^T \\
&= \sum_{m=1}^{\infty} \{u_m(x), w_m(x), \varphi_{\theta_m}(x), N_{x_m}(x), Q_{x_m}(x), M_{x_m}(x)\}^T \cos m\theta e^{i\omega t}, \\
&\{v_0(x, \theta, t), \varphi_x(x, \theta, t), N_{x\theta}(x, \theta, t), M_{x\theta}(x, \theta, t)\}^T \\
&= \sum_{m=1}^{\infty} \{v_m(x), \varphi_{x_m}(x), N_{x\theta_m}(x), M_{x\theta_m}(x)\}^T \sin m\theta e^{i\omega t},
\end{aligned} \tag{13}$$

where  $m$  is the number of circumferential wave. Substituting (13) in equations (12) and (10), a system of ordinary differential equations in the  $x$ -coordinate for the  $m^{\text{th}}$  mode can be expressed in the matrix form for each circumferential mode  $m$  as [9]

$$\begin{aligned}
\frac{du_m}{dx} &= c_4 \sin \alpha .u_m + mc_4 v_m + c_4 \cos \alpha .w_m + c_5 \sin \alpha .\varphi_{xm} + mc_5 \varphi_{\theta m} + \frac{D_{11}}{c_1} N_{xm} - \frac{B_{11}}{c_1} M_{xm}, \\
\frac{dv_m}{dx} &= \frac{m}{R(x)} u_m + \frac{\sin \alpha}{R(x)} v_m - \frac{D_{66}}{c_{10}} N_{x\theta m} + \frac{B_{66}}{c_{10}} M_{x\theta m}, \\
\frac{dw_m}{dx} &= -\varphi_{xm} + \frac{1}{fF_{55}} Q_{xm}, \\
\frac{d\varphi_{xm}}{dx} &= c_2 \sin \alpha .u_m + mc_2 v_m + c_2 \cos \alpha .w_m + c_3 \sin \alpha .\varphi_{xm} + mc_3 \varphi_{\theta m} - \frac{B_{11}}{c_1} N_{xm} + \frac{A_{11}}{c_1} M_{xm}, \\
\frac{d\varphi_{\theta m}}{dx} &= \frac{m}{R(x)} \varphi_{xm} + \frac{\sin \alpha}{R(x)} \varphi_{\theta m} + \frac{B_{66}}{c_{10}} N_{x\theta m} - \frac{A_{66}}{c_{10}} M_{x\theta m}, \\
\frac{dN_{xm}}{dx} &= (c_6 \sin^2 \alpha - I_0 \omega^2) u_m + mc_6 \sin \alpha .v_m + c_6 \sin \alpha \cos \alpha .w_m + (c_7 \sin^2 \alpha - I_1 \omega^2) \varphi_{xm} \\
&\quad + mc_7 \sin \alpha .\varphi_{\theta m} - \sin \alpha \left( c_4 + \frac{1}{R(x)} \right) N_{xm} - \frac{m}{R(x)} N_{x\theta m} - c_2 \sin \alpha .M_{xm}, \\
\frac{dN_{x\theta m}}{dx} &= mc_6 \sin \alpha .u_m + \left( m^2 c_6 + \frac{fF_{44} \cos^2 \alpha}{R(x)^2} - I_0 \omega^2 \right) v_m + m \cos \alpha \left( c_6 + \frac{fF_{44}}{R(x)^2} \right) w_m + \\
&\quad + mc_7 \sin \alpha .\varphi_{xm} + \left( m^2 c_7 - \frac{fF_{44} \cos \alpha}{R(x)} - I_1 \omega^2 \right) \varphi_{\theta m} - mc_4 N_{xm} - \frac{2 \sin \alpha}{R(x)} N_{x\theta m} - mc_2 M_{xm}, \\
\frac{dQ_{xm}}{dx} &= c_{13} \left( c_1 \sin \alpha + \frac{A_{11}}{R(x)^2} \cos \alpha + k_p c_2 \sin \alpha \right) u_m + mc_{13} \left( \frac{fF_{44}}{R(x)^2} \cos \alpha + c_{11} + \frac{A_{11}}{R(x)^2} \cos \alpha + k_p c_2 \right) v_m \quad (14) \\
&\quad + c_{13} \left( \frac{m^2 fF_{44}}{R(x)^2} + c_{11} \cos \alpha + k_p c_2 \cos \alpha - I_0 \omega^2 + k_w + \frac{m^2 k_p}{R(x)^2} \right) w_m \\
&\quad + c_{13} \left( c_{12} \sin \alpha + \frac{B_{22}}{R(x)^2} \cos \alpha + k_p \frac{\sin \alpha}{R(x)} + k_p c_3 \sin \alpha \right) \varphi_{xm} \\
&\quad + mc_{13} \left( -\frac{fF_{44}}{R(x)} + c_{12} + \frac{B_{22}}{R(x)^2} \cos \alpha + k_p c_3 \right) \varphi_{\theta m} \\
&\quad + c_{13} \left( \frac{A_{12}}{R(x)} \frac{D_{11}}{c_1} \cos \alpha - \frac{B_{12}}{R(x)} \frac{B_{11}}{c_1} \cos \alpha - k_p \frac{B_{11}}{c_1} \right) N_{xm} - \frac{\sin \alpha}{R(x)} Q_{xm} \\
&\quad + c_{13} \left( -\frac{A_{12}}{R(x)} \frac{B_{11}}{c_1} \cos \alpha + \frac{B_{12}}{R(x)} \frac{A_{11}}{c_1} \cos \alpha + k_p \frac{A_{11}}{c_1} \right) M_{xm}, \\
\frac{dM_{xm}}{dx} &= (2c_8 \sin^2 \alpha - I_1 \omega^2) u_m + 2mc_8 \sin \alpha .v_m + 2c_8 \sin \alpha \cos \alpha .w_m + (2c_9 \sin^2 \alpha - I_2 \omega^2) \varphi_{xm} \\
&\quad + 2mc_9 \sin \alpha .\varphi_{\theta m} - 2c_5 \sin \alpha .N_{xm} + Q_x - \left[ 2 \sin \alpha \left( c_3 + \frac{1}{R(x)} \right) \right] M_{xm} - \frac{m}{R} M_{x\theta m}, \\
\frac{dM_{x\theta m}}{dx} &= mc_8 \sin \alpha .u_m + \left( m^2 c_8 - \frac{fF_{44} \cos \alpha}{R(x)} - I_1 \omega^2 \right) v_m + m \left( c_8 \cos \alpha - \frac{fF_{44}}{R(x)} \right) w_m \\
&\quad + mc_9 \sin \alpha .\varphi_{xm} + \left( m^2 c_9 + fF_{44} - I_2 \omega^2 \right) \varphi_{\theta m} - mc_5 N_{xm} - mc_3 M_{xm} - \frac{2 \sin \alpha}{R(x)} M_{x\theta m},
\end{aligned}$$

with

$$\begin{aligned}
c_1 &= A_{11} D_{11} - B_{11}^2, \quad c_2 = (A_{12} B_{11} - A_{11} B_{12}) / R(x) c_1, \\
c_3 &= (B_{11} B_{12} - A_{11} D_{12}) / R(x) c_1, \quad c_4 = (B_{11} B_{12} - A_{12} D_{11}) / R(x) c_1, \\
c_5 &= (B_{11} D_{12} - B_{12} D_{11}) / R(x) c_1, \quad c_6 = (A_{12} c_4 + B_{12} c_2 + A_{22} / R(x)) / R(x), \\
c_7 &= (A_{12} c_5 + B_{12} c_3 + B_{22} / R(x)) / R(x), \quad c_8 = (B_{12} c_4 + D_{12} c_2 + B_{22} / R(x)) / R(x),
\end{aligned}$$

$$c_9 = (B_{12}c_5 + D_{12}c_3 + D_{22}/R(x)) / R(x), \quad c_{10} = B_{66}^2 - A_{66}D_{66},$$

$$c_{11} = \frac{A_{12}}{R(x)}c_4 \cos \alpha + \frac{B_{12}}{R(x)}c_2 \cos \alpha, \quad c_{12} = \frac{A_{12}}{R(x)}c_5 \cos \alpha + \frac{B_{12}}{R(x)}c_3 \cos \alpha, \quad c_{13} = \frac{1}{1 + \frac{k_p}{fF55}}.$$

Eq. (14) can be expressed in the matrix form for each circumferential mode  $m$

$$\frac{d\mathbf{y}_m}{dx} = A_m \mathbf{y}_m, \quad (15)$$

with  $A_m$  is a  $10 \times 10$  matrix (see Appendix). The dynamic transfer matrix  $T_m$  is evaluated as

$$T_m(\omega) = e^{\int_0^L A_m(\omega) dx} = \begin{bmatrix} T_{11} & T_{12} \\ T_{21} & T_{22} \end{bmatrix}. \quad (16)$$

Finally, the dynamic stiffness matrix  $K_m(\omega)$  for FG truncated conical shell is determined by [8]

$$K_m(\omega) = \begin{bmatrix} T_{12}^{-1}T_{11} & -T_{12}^{-1} \\ T_{21} - T_{22}T_{12}^{-1}T_{11} & T_{22}T_{12}^{-1} \end{bmatrix}. \quad (17)$$

Natural frequencies will be extracted from the harmonic responses of the structure by using the procedure developed in [8,9].

#### 4. CONTINUOUS ELEMENT FOR FG STEPPED TRUNCATED CONICAL SHELLS

Let's investigate a stepped conical shell (SCS) including  $n$  segments shown in Fig. 3. The SCS consists of  $n$  lengths  $L_1, L_2, \dots, L_i, \dots, L_n$  and  $n$  step thicknesses  $h_1, h_2, \dots, h_i, \dots, h_n$ . Let the coordinate system be chosen as shown in Fig. 2;  $\theta$  is the circumferential coordinate,  $R_1$  and  $R_2$  are the respectively small radius and large cone surface, the cone semi-vertex angle ( $\alpha$ ) of the steps are the same;  $u, v$  and  $w$  are the displacement components in the  $x, \theta$  and normal directions, respectively.

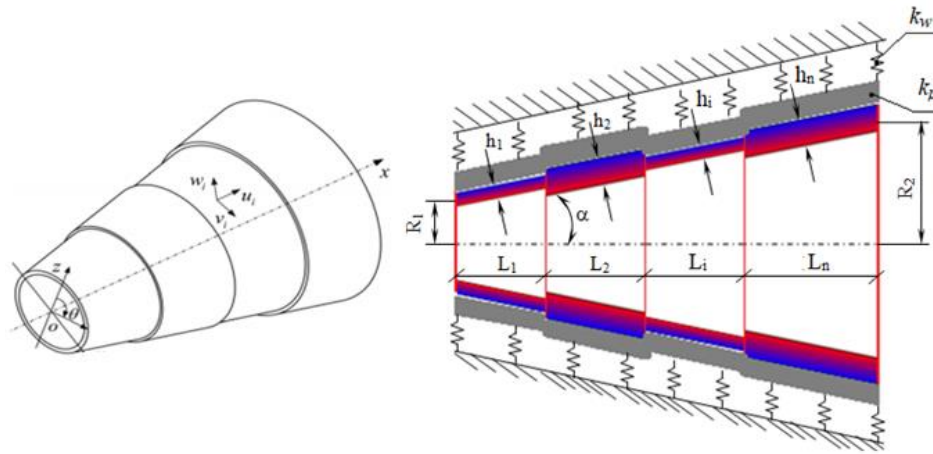


Fig. 3. Geometry of a FG stepped truncated conical shells

The dynamic stiffness matrix  $K_m(\omega)$  for the above FG stepped truncated conical shells surrounded by elastic foundation will be constructed by assembling the DSM of various segments having different constant thickness and lengths. First, the shell is divided into  $n$  elements. It is necessary to build  $n$  separate dynamic stiffness matrices  $K_{seg1}, K_{seg2}, \dots, K_{segi}, \dots, K_{segn}$  for these segments. Then, Fig. 4 describes the assembly procedure for constructing the DSM for the stepped conical shells. The natural frequencies of the studied structure will be determined from this matrix by using the method detailed in [8].

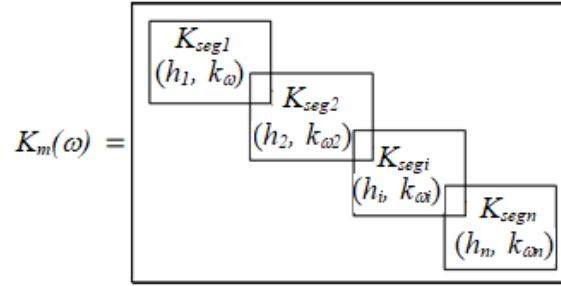


Fig. 4. Construction of the dynamic stiffness matrix for FG stepped truncated conical shells

The procedure of combining the dynamic stiffness matrix  $K(\omega)_m$  for stepped conical shell is based on the continuous condition at the joints between segments of the shell. In this study, we only investigated the conical shell with segments having the same conical angle. Thus, all shell segments have neutral faces overlapping and the continuous condition at the position of the coupling between the segments of the shells as follows

$$\begin{aligned} u_i &= u_{i+1}, & v_i &= v_{i+1}, & w_i &= w_{i+1}, \\ N_x^i &= N_x^{i+1}, & N_{x\theta}^i &= N_{x\theta}^{i+1}, & Q_x^i &= Q_x^{i+1}, \\ M_{x\theta}^i &= M_{x\theta}^{i+1}, & M_x^i &= M_x^{i+1}. \end{aligned} \quad (18)$$

## 5. NUMERICAL RESULTS AND DISCUSSION

The present exact procedure may be applied to investigate the effects of various geometrical and material properties such as step thickness ratios, the power law index and different boundary conditions. Four configuration of functionally graded material are used with the material properties listed in Tab. 1.

Table 1. Material properties of functionally graded materials

Properties	FGM1		FGM2		FGM3		FGM4	
	Al	Zirconia	Al	Alloy	Al	Al <sub>2</sub> O <sub>3</sub>	Nickel	Si3N4
E (GPa)	70	168	70	211	70	380	205.098	322.27
$\mu$	0.3	0.3	0.3	0.3	0.3	0.3	0.31	0.24
$\rho$ (kg/m <sup>3</sup> )	2707	5700	2707	7800	2707	3800	8900	2370

**5.1. Validation of the present model**

The proposed continuous element model will be validated by comparison with solutions available in the literature with finite element results and other methods. First, to check the accuracy of the present method on the vibration analysis of FGM conical shells, Tabs. 2 and 3 show the first frequencies for FGM (Si3N4/Ni) conical shells with different values of  $k_w, k_p$ . The geometrical parameters of the FGM conical shells are  $R_1/h = 100; h = 0.01; L = 2R_1; \alpha = 30^\circ$ .

Table 2. Comparison dimensionless frequency parameter for FGM conical shells resting on the Winkler–Pasternak foundations with moduli  $k_w$  and  $k_p$  different and F-C boundary conditions

$k_w$ (N/m <sup>3</sup> )	$k_p$ (N/m)	FGM4 <sub>I(a=1/b=0/c=2/p=∞)</sub>			FGM4 <sub>I(a=1/b=0/c=2/p=1)</sub>			FGM4 <sub>I(a=1/b=0/c=2/p=2)</sub>		
		Sofiyev [4]	CEM	Difference	Sofiyev [4]	CEM	Difference	Sofiyev [4]	CEM	Difference
0	0	0.0723	0.0699	3.35	0.0997	0.0970	2.71	0.0887	0.0855	3.58
$5 \times 10^6$	0	0.0813	0.0782	3.78	0.1103	0.1085	1.66	0.0988	0.0970	1.82
	$1 \times 10^5$	0.0845	0.0814	3.72	0.1146	0.1116	2.62	0.1024	0.1001	2.22
	$2.5 \times 10^5$	0.0888	0.0866	2.51	0.1198	0.1179	1.62	0.1072	0.1053	1.73
	$5 \times 10^5$	0.0956	0.0939	1.81	0.1279	0.1262	1.33	0.1148	0.1137	0.97
$1 \times 10^7$	0	0.0894	0.0876	2.00	0.1200	0.1189	0.91	0.1078	0.1064	1.31
	$1 \times 10^5$	0.0923	0.0897	2.82	0.1240	0.1220	1.59	0.1112	0.1095	1.52
	$2.5 \times 10^5$	0.0963	0.0949	1.44	0.1287	0.1272	1.13	0.1156	0.1147	0.75
	$5 \times 10^5$	0.1025	0.1012	1.30	0.1363	0.1356	0.52	0.1227	0.1220	0.55
$5 \times 10^7$	0	0.1380	0.1398	1.28	0.1797	0.1815	0.99	0.1631	0.1648	1.04
	$1 \times 10^5$	0.1399	0.1418	1.39	0.1823	0.1836	0.70	0.1653	0.1669	0.96
	$2.5 \times 10^5$	0.1426	0.1439	0.94	0.1856	0.1867	0.59	0.1684	0.1700	0.96
	$5 \times 10^5$	0.1469	0.1491	1.53	0.1910	0.1930	1.02	0.1733	0.1752	1.11

Tabs. 2 and 3 presented the variations of the dimensionless fundamental natural frequency for the FG truncated conical shells with different  $k_w, k_p$  coefficients. It is observed that dimensionless frequency parameter of FG truncated conical shells increases gradually with the increasing of  $k_w$  or  $k_p$ . We see that for their small to intermediate values, both Winkler and shearing layer elastic coefficients have significant effects on the dimensionless fundamental natural frequency. However, for the large values of the Winkler elastic coefficient, the shearing layer elastic coefficient has negligible effect on dimensionless frequency.

Natural frequencies computed by CEM are compared with those of Sofiyev and Schnack [4] and obtained differences vary from 0.37% to 4.67%. Therefore, this continuous element model is reliable and effective to study FGM truncated conical shells surrounded by Pasternak elastic foundations.

Next, the frequency parameters of a four-stepped conical shell are listed in Tab. 4. The dimensional parameters are: semi-vertex angles  $\alpha_1 = \alpha_2 = \alpha_3 = \alpha_4 = 18^\circ$ , thickness ratios  $h_1 : h_2 = 1/2, h_1 : h_3 = 1/3, h_1 : h_4 = 1/4$ , length ratios  $L_1 : L_2 = 1, L_1 : L_3 = 1, L_1 : L_4 = 1$ , thickness of the first segment  $h_1 = 0.01$  m, radii of two ends  $R_1 = 0.5$  m,  $R_2 = 1$  m. For all modes presented in this table, the discrepancy of frequency parameters of presented model and those from literature is negligible. In addition, frequency parameters of a finite element model developed in ANSYS are also tabulated. SHELL181

Table 3. Comparison of the lowest dimensionless frequency parameter for FGM conical shells resting on the Winkler–Pasternak foundations with moduli  $k_w$  and  $k_p$  different and F-C boundary conditions

$k_w$ (N/m <sup>3</sup> )	$k_p$ (N/m)	FGM4 <sub>II(a=1/b=0/c=2/p=2)</sub>		Difference	FGM4 <sub>I(a=1/b=0/c=2/p=0)</sub>		Difference
		Sofiyev [4]	CEM		Sofiyev [4]	CEM	
0	0	0.1139	0.1116	2.02	0.1763	0.1690	4.16
$5 \times 10^6$	0	0.1255	0.1241	1.10	0.1910	0.1825	4.44
	$1 \times 10^5$	0.1306	0.1283	1.77	0.1974	0.1877	4.89
	$2.5 \times 10^5$	0.1362	0.1335	1.98	0.2046	0.1950	4.67
	$5 \times 10^5$	0.1451	0.1429	1.52	0.2162	0.2076	4.00
$1 \times 10^7$	0	0.1361	0.1356	0.37	0.2047	0.1971	3.70
	$1 \times 10^5$	0.1408	0.1387	1.48	0.2106	0.2023	3.92
	$2.5 \times 10^5$	0.1460	0.1450	0.70	0.2175	0.2086	4.09
	$5 \times 10^5$	0.1543	0.1533	0.63	0.2284	0.2211	3.19
$5 \times 10^7$	0	0.2017	0.2044	1.35	0.2918	0.2889	0.99
	$1 \times 10^5$	0.2049	0.2065	0.79	0.2960	0.2920	1.34
	$2.5 \times 10^5$	0.2085	0.2107	1.05	0.3009	0.2973	1.21
	$5 \times 10^5$	0.2144	0.2159	0.70	0.3089	0.3056	1.07

Difference (%) = |(CEM – Sofiyev)/Sofiyev| × 100.

Table 4. Comparisons of frequency parameters for a four-stepped conical shell with different thickness and F-C boundary conditions (FGM2<sub>I(a=1/b=0/c=2/p=0)</sub>)

$n$	$m$	Qu et al. [7]	Xie et al. [6]	Anslys	CEM	Differences (%)
0	1	1.0560	1.0561	1.0540	1.0281	2.64
	2	1.0876	1.0873	1.0851	1.1385	4.68
	3	1.2156	1.2151	1.2123	1.2535	3.12
	4	1.3493	1.3490	1.3458	1.3547	0.40
	5	1.3796	1.3792	1.3756	1.4686	6.45
	6	1.4990	1.4986	1.4946	1.5525	3.57
1	1	0.6240	0.6240	0.6226	0.6808	9.10
	2	0.9848	0.9845	0.9823	0.9361	4.95
	3	1.1397	1.1391	1.1367	1.1075	2.83
	4	1.3050	1.3044	1.3012	1.2524	4.03
	5	1.4203	1.4196	1.4158	1.3685	3.65
	6	1.5529	1.5528	1.5487	1.4847	4.40
2	1	0.3372	0.3369	0.3361	0.3542	5.04
	2	0.6610	0.6606	0.6591	0.6590	0.31
	3	0.9483	0.9477	0.9457	0.9269	2.26
	4	1.1456	1.1447	1.1423	1.1098	3.13
	5	1.3554	1.3543	1.3511	1.2972	4.29
	6	1.5261	1.5251	1.5211	1.4571	4.52

Difference (%) = |(CEM – Qu [7])/Qu [7]| × 100.

elements are employed for the finite element model and the shell is uniformly meshed into 160 and 80 elements in circumferential and meridional direction, which satisfies the requirement of convergence. It can be observed that frequency parameters of ANSYS model show well agreement with those of literature and with the present method. This demonstrates the validity of the CEM model.

**5.2. Effect of parameters on the natural frequency**

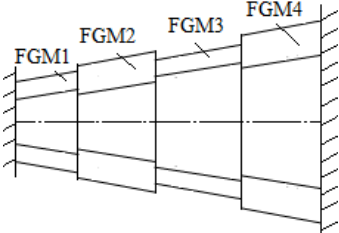
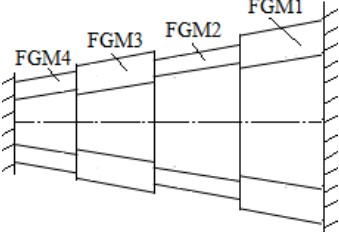
In this section, the influences of various shell parameters and elastic foundations on the dynamic behavior of the stepped conical shells will be studied such as stepped thickness configurations, boundary conditions. Different stiffness values of  $k_w, k_p$  are also taken into account.

**5.2.1. Effect of geometric parameters**

First, Tab. 5 has shown the first eight natural frequencies of the Clamped-Clamped (C-C) of a four-stepped conical shell with  $R_1 = 0.5; R_2 = 1$  m,  $h_1 : h_2 : h_3 : h_4 = 1 : 2 : 3 : 4; L_1 : L_2 : L_3 : L_4 = 1 : 1 : 1 : 1; h_1 = 0.01$  m,  $FGM_{I(a=1/b=0.5/c=1/p=2)}$ . In Tab. 5, the increase of the semi-vertex angle augments the stiffness of the structure, resulting in an increasing of natural frequencies. The variation of material properties of each segment also changes the natural frequency of the shell.

Next, the effect of stepped thickness on free vibration of FG stepped truncated conical shells will be analyzed in detail. The considered stepped conical shell is subjected to the clamped-clamped boundary condition and has the following dimensions:  $L_1 : L_2 : L_3 : L_4 = 1 : 1 : 1 : 1, R_1 = 0.5, R_2 = 1, h_1 = 0.01$  m,  $\alpha = 18^\circ, FGM_{I(a=1/b=0/c=2/p=0)}$ ,

Table 5. Effect of a semi-vertex angle and variation of FGM material at steppeds of the shell

Frequency (Hz)	Change of FGM materials at steppeds	Semi-vertex angle ( $\alpha$ )		
		10°	18°	30°
$f_1$	FGM1/FGM2/FGM3/FGM4	188	324	507
$f_2$		201	352	517
$f_3$		266	383	562
$f_4$		281	430	608
$f_5$		330	535	661
$f_6$		350	557	780
$f_7$		368	584	788
$f_8$		380	604	906
$f_1$		FGM4/FGM3/FGM2/FGM1	183	316
$f_2$		206	357	503
$f_3$		261	360	560
$f_4$		288	458	576
$f_5$		306	493	692
$f_6$		349	538	696
$f_7$		353	557	840
$f_8$		397	588	849

Material 1 is used and the elastic foundation stiffness is  $k_w, k_p = 0$ . Here, four different configurations of stepped thickness are examined:  $h_1 : h_2 : h_3 : h_4 = 1 : 2 : 3 : 4 / 2 : 2 : 3 : 4 / 3 : 2 : 3 : 4 / 4 : 2 : 3 : 4 / 4 : 3 : 2 : 1$  and results are summarized in Fig. 5. It can be seen that except the first three modes, the augmentation of the stepped thickness leads to the raise of natural frequencies of all other circumferential modes ( $m$ ). In addition, the effect of the thickness of segments on the first mode is minimal.

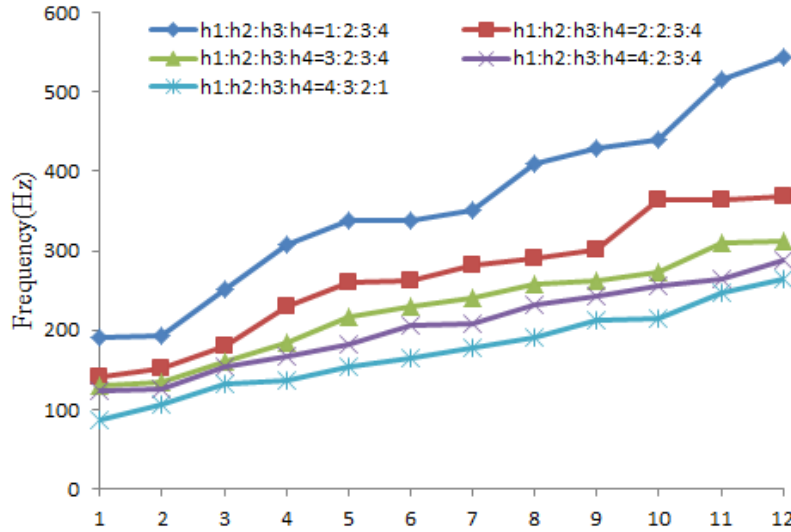


Fig. 5. Effect of stepped thickness on the vibration of four-FG stepped truncated conical shells

### 5.2.2. Influences of elastic foundations

It is necessary to examine the effects of different types of elastic foundations on the free vibration of the FG stepped truncated conical shells. Consider now the above mentioned four-stepped conical shell surrounded by a Winkler foundation with various values of foundation stiffness  $k_w$ . The parameters of the shell are as follows:  $h_1 : h_2 : h_3 : h_4 = 1 : 2 : 1 : 2, h_1 = 0.01 \text{ m}, L_1 : L_2 : L_3 : L_4 = 1 : 1 : 1 : 1, R_1 = 0.5 \text{ m}; R_2 = 1 \text{ m}, \alpha = 20^\circ$ , material properties at steps 1, 2, 3, 4 are FGM1, FGM2, FGM4 and FGM3, respectively.

Six different values of  $k_w$  ( $0, 2.5 \times 10^4, 5 \times 10^6, 2.5 \times 10^7, 5 \times 10^8, 10^9 \text{ N/m}^3$ ) are taken for the study and results are illustrated in Fig. 6. It is easy to remark that when  $k_w \leq 2.5 \times 10^7 \text{ N/m}^3$  the effects of Winkler foundation stiffness on natural frequency are very small. When the stiffness of the Winkler foundation  $k_w \geq 5 \times 10^8 \text{ N/m}^3$ , the natural frequency of the shell increases as  $k_w$  increases and then the effect of  $k_w$  on the natural frequency is obvious.

The effect of Pasternak foundations has been investigated in the next test case. The same structure resting on a Pasternak foundation with  $k_w = 5 \times 10^6 \text{ N/m}^3$  and various values of shear stiffness are chosen:  $k_p = 10^2, 2.5 \times 10^4, 5 \times 10^6, 2.5 \times 10^7, 10^8 \text{ (N/m)}$ . Fig. 7 presents the variation of natural frequencies of the studied structure with respect

to different values of the shear stiffness  $k_p$ . It is observed from this figure that natural frequencies increase rapidly as  $k_p > 5 \times 10^6$  N/m. When  $m$  increases, the influence of Pasternak foundation on natural frequency becomes larger. With  $k_p \leq 2.5 \times 10^4$  N/m, Pasternak foundations have almost no effects on the natural frequencies of the shell.

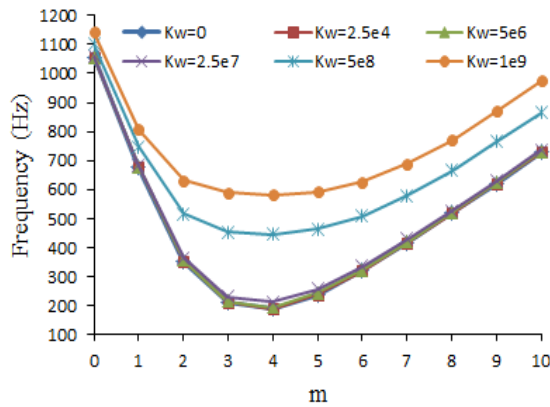


Fig. 6. Influence of Winkler foundations on natural frequencies of four-FGM<sub>I(a=1/b=0.5/c=4/p=2)</sub> stepped truncated conical shell with F-C boundary conditions

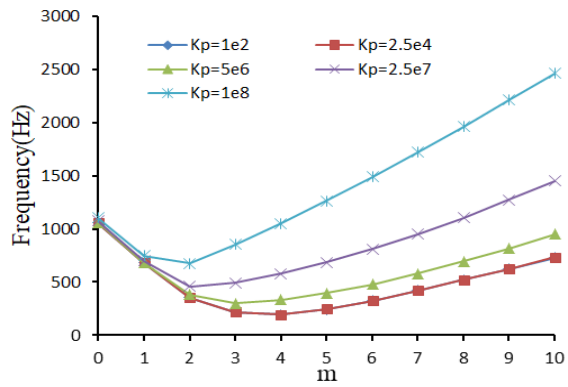


Fig. 7. Influence of Pasternak foundations on natural frequencies of four-FGM<sub>I(a=1/b=0.5/c=4/p=2)</sub> stepped truncated conical shell with F-C boundary conditions

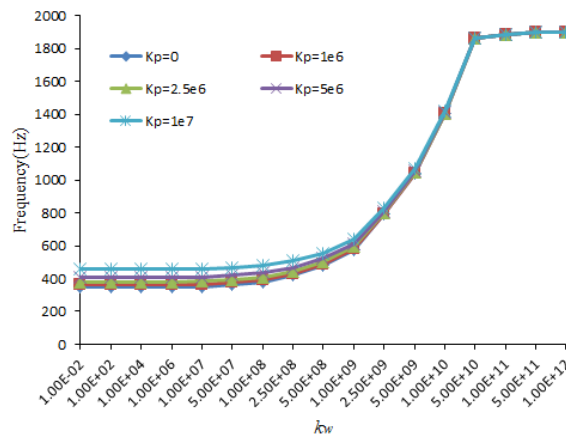


Fig. 8. Influences of both Winkler stiffness and Pasternak stiffness to natural frequencies of four-FGM<sub>I(a=1/b=0.5/c=1/p=4)</sub> stepped truncated conical shell with S-S boundary conditions

Next, effects of both Winkler stiffness and Pasternak stiffness on natural frequencies of four-FG stepped truncated conical shells will be studied and illustrated in Fig. 8. The parameters of the shell are as follows:  $h_1 : h_2 : h_3 : h_4 = 1 : 2 : 3 : 4$ ,  $h_1 = 0.01$  m,  $L_1 : L_2 : L_3 : L_4 = 1 : 1 : 1 : 1$ ,  $R_1 = 0.5$  m;  $R_2 = 1$  m,  $\alpha = 20^\circ$ , material properties at steps 1, 2, 3, 4 are FGM1, FGM2, FGM4 and FGM3, respectively. The values of Winkler

stiffness and Pasternak stiffness are  $k_w = 10^{-2}, 10^2, 10^4, 10^6, 10^7, 5 \times 10^7, 10^8, 2.5 \times 10^8, 5 \times 10^8, 10^9, 2.5 \times 10^9, 5 \times 10^9, 10^{10}, 5 \times 10^{10}, 10^{11}, 5 \times 10^{11}, 10^{12}$  N/m<sup>3</sup> and  $k_p = 0, 10^6, 2.5 \times 10^6, 5 \times 10^6, 10^7$  N/m, respectively. From Fig. 8, it can be seen that the effect of Winkler stiffness and Pasternak stiffness on natural frequencies is important only on a certain range ( $k_w$  from  $10^7$  to  $10^{11}$  N/m<sup>3</sup>,  $k_p$  from  $5 \times 10^6$  to  $10^8$  N/m). When  $k_w$  reaches to the limit value  $k_w = 10^{12}$  N/m<sup>3</sup>, Pasternak stiffness values have less effect on natural frequencies.

5.2.3. Influence of the power-law  $p$  and various values of the parameter  $b$

In Fig. 9 the variation of first four frequencies of four-step functionally graded conical shell (F-C) versus the power-law index  $p$  for two power-law distributions and for various values of the parameter  $b$  ( $b$  is contained in the interval  $[0, 1]$ ) are presented. The parameters of the shell are as follows:  $h_1 : h_2 : h_3 : h_4 = 1 : 2 : 3 : 4, h_1 = 0.01$  m,  $L_1 : L_2 : L_3 : L_4 = 1 : 1 : 1 : 1, R_1 = 0.5$  m;  $R_2 = 1$  m,  $\alpha = 30^\circ$ ,  $FGM_{I(a=1/0 \leq b \leq 1/c=3/p)}$ , material properties at steps 1, 2, 3, 4 are FGM1, FGM2, FGM4 and FGM3, respectively. As can be seen from Fig. 9, natural frequencies of FGM shells often present an intermediate

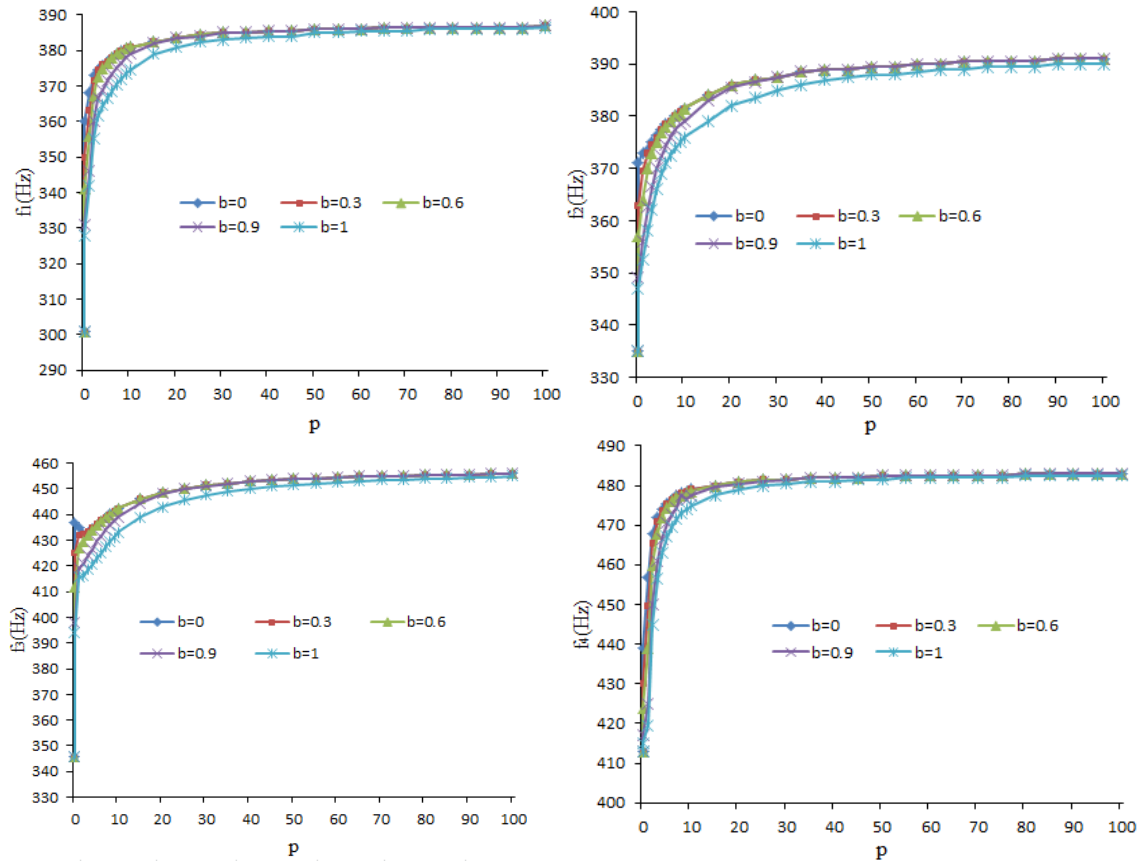


Fig. 9. First four frequencies of four-FG stepped truncated conical shell (F-C) versus the power-law exponent  $p$  for various values of the parameter  $b$

value between the natural frequencies of the limit cases of homogeneous shells of zirconia  $p = 0$  and of aluminum  $p = \infty$ , as expected. However, natural frequencies sometimes exceed limit cases, this fact can depend on various parameters, such as the geometry of the shell, the boundary conditions, the power-law distribution profile, etc.

## 6. CONCLUSIONS

This research has succeeded in constructing a Continuous Element model for Functional Graded stepped truncated conical shells made of various materials and surrounded by Winkler and Pasternak elastic foundations. The effect of the Pasternak elastic foundation and of Function Graded Material have been well integrated into the presented element. Good agreements are noticed between the results obtained by our approach and those of other methods. Numerical results have confirmed that Continuous Element model is accurate and economizes the storage capacity of computers by using a minimum meshing. The effects of various parameters on vibration behavior of the stepped shell are also investigated. From the above results, it can be concluded that:

1. The ratio thickness-to-radius has a larger effect on natural frequencies when  $m$  increases ( $m > 1$ ).

2. The stiffness parameters of the elastic foundation have a significant effect on the vibration of the FG stepped truncated conical shells. As the stiffness parameters are greater, the frequencies are higher.

3. For the FG stepped truncated conical shells surrounded by elastic foundation, the effect of Winkler stiffness and Pasternak stiffness on natural frequency is noticeable in a certain range. When the Winkler stiffness reaches a limited value (as  $k_w = 10^{12}$  N/m<sup>3</sup>), the influence of shearing layer elastic stiffness parameter in natural frequency is hardly recognized.

The developed continuous element model with its powerful assembling procedure can be expanded to study more complex shell structures such as: joined cylindrical-conical shells, combined cylindrical-conical shell and annular plates, ring-stiffened shells and those structures surrounded by elastic foundations and fluid.

## ACKNOWLEDGEMENT

This research is funded by Vietnam National Foundation for Science and Technology Development (NAFOSTED) under Grant number: 107.02-2018.07.

## REFERENCES

- [1] P. L. Pasternak. On a new method of analysis of an elastic foundation by means of two foundation constants. *Gos. Izd. Lit. po Stroitu I Arkh. Moscow, USSR*, (1954). (in Russian).
- [2] A. D. Kerr. Elastic and viscoelastic foundation models. *Journal of Applied Mechanics*, **31**, (3), (1964), pp. 491–498. <https://doi.org/10.1115/1.3629667>.
- [3] A. H. Sofiyev and N. Kuruoglu. Vibration analysis of FGM truncated and complete conical shells resting on elastic foundations under various boundary conditions. *Journal of Engineering Mathematics*, **77**, (1), (2012), pp. 131–145. <https://doi.org/10.1007/s10665-012-9535-3>.

- [4] A. H. Sofiyev and E. Schnack. The vibration analysis of FGM truncated conical shells resting on two-parameter elastic foundations. *Mechanics of Advanced Materials and Structures*, **19**, (4), (2012), pp. 241–249. <https://doi.org/10.1080/15376494.2011.642934>.
- [5] H. L. K. Dung, Dao Van and N. T. Nga. On the stability of functionally graded truncated conical shells reinforced by functionally graded stiffeners and surrounded by an elastic medium. *Composite Structures*, **108**, (2014), pp. 77–90. <https://doi.org/10.1016/j.compstruct.2013.09.002>.
- [6] K. Xie, M. Chen, and Z. Li. An analytic method for free and forced vibration analysis of stepped conical shells with arbitrary boundary conditions. *Thin-Walled Structures*, **111**, (2017), pp. 126–137. <https://doi.org/10.1016/j.tws.2016.11.017>.
- [7] Y. Qu, Y. Chen, Y. Chen, X. Long, H. Hua, and G. Meng. A domain decomposition method for vibration analysis of conical shells with uniform and stepped thickness. *Journal of Vibration and Acoustics*, **135**, (1), (2013). <https://doi.org/10.1115/1.4006753>.
- [8] L. Q. Vinh, N. M. Cuong, and L. T. B. Nam. Dynamic analysis of stepped composite conical shells via continuous element method. In *2nd National Conference on Mechanical Engineering and Automation*, Hanoi, Vietnam, (2016), pp. 338–344.
- [9] L. T. B. Nam, N. M. Cuong, T. I. Tran, and L. Q. Vinh. Dynamic analysis of stepped composite cylindrical shells surrounded by Pasternak elastic foundations based on the continuous element method. *Vietnam Journal of Mechanics*, **40**, (2), (2018), pp. 105–119. <https://doi.org/10.15625/0866-7136/9832>.

## APPENDIX

Matrix  $[A(\omega)]_{10 \times 10}$ :

$$A_{xm} = \begin{bmatrix} A_{11} & A_{12} & A_{13} & A_{14} & A_{15} & A_{16} & A_{17} & A_{18} & A_{19} & A_{110} \\ A_{21} & A_{22} & A_{23} & A_{24} & A_{25} & A_{26} & A_{27} & A_{28} & A_{29} & A_{210} \\ A_{31} & A_{32} & A_{33} & A_{34} & A_{35} & A_{36} & A_{37} & A_{38} & A_{39} & A_{310} \\ A_{41} & A_{42} & A_{43} & A_{44} & A_{45} & A_{46} & A_{47} & A_{48} & A_{49} & A_{410} \\ A_{51} & A_{52} & A_{53} & A_{54} & A_{55} & A_{56} & A_{57} & A_{58} & A_{59} & A_{510} \\ A_{61} & A_{62} & A_{63} & A_{64} & A_{65} & A_{66} & A_{67} & A_{68} & A_{69} & A_{610} \\ A_{71} & A_{72} & A_{73} & A_{74} & A_{75} & A_{76} & A_{77} & A_{78} & A_{79} & A_{710} \\ A_{81} & A_{82} & A_{83} & A_{84} & A_{85} & A_{86} & A_{87} & A_{88} & A_{89} & A_{810} \\ A_{91} & A_{92} & A_{93} & A_{94} & A_{95} & A_{96} & A_{97} & A_{98} & A_{99} & A_{910} \\ A_{101} & A_{102} & A_{103} & A_{104} & A_{105} & A_{106} & A_{107} & A_{108} & A_{109} & A_{1010} \end{bmatrix},$$

$$\begin{aligned} A_{11} &= c_4 \sin \alpha, & A_{12} &= mc_4, & A_{13} &= c_4 \cos \alpha, & A_{14} &= c_5 \sin \alpha, \\ A_{15} &= mc_5, & A_{16} &= \frac{D_{11}}{c_1}, & A_{17} &= 0, & A_{18} &= 0, & A_{19} &= -\frac{B_{11}}{c_1}, & A_{110} &= 0, \\ A_{21} &= \frac{m}{R(x)}, & A_{22} &= \frac{\sin \alpha}{R(x)}, & A_{23} &= 0, & A_{24} &= 0, & A_{25} &= 0, & A_{26} &= 0, \\ A_{27} &= -\frac{D_{66}}{c_{10}}, & A_{28} &= 0, & A_{29} &= 0, & A_{210} &= -\frac{B_{66}}{c_{10}}, \\ A_{31} &= 0, & A_{32} &= 0, & A_{33} &= 0, & A_{34} &= -1, & A_{35} &= 0, & A_{36} &= 0, \\ A_{37} &= 0, & A_{38} &= \frac{1}{fF_{55}}, & A_{39} &= 0, & A_{310} &= 0, \\ A_{41} &= c_2 \sin \alpha, & A_{42} &= mc_2, & A_{43} &= c_2 \cos \alpha, & A_{44} &= c_3 \sin \alpha, & A_{45} &= mc_3, \\ A_{46} &= -\frac{B_{11}}{c_1}, & A_{47} &= 0, & A_{48} &= 0, & A_{49} &= \frac{A_{11}}{c_1}, & A_{410} &= 0, \\ A_{51} &= 0, & A_{52} &= 0, & A_{53} &= 0, & A_{54} &= \frac{m}{R(x)}, & A_{55} &= \frac{\sin \alpha}{R(x)}, & A_{56} &= 0, \\ A_{57} &= \frac{B_{66}}{c_{10}}, & A_{58} &= 0, & A_{59} &= 0, & A_{510} &= -\frac{A_{66}}{c_{10}}, \\ A_{61} &= c_6 \sin \alpha - I_0 \omega^2, & A_{62} &= mc_6 \sin \alpha, & A_{63} &= c_6 \sin \alpha \cos \alpha, \\ A_{64} &= c_7 \sin^2 \alpha - I_1 \omega^2, & A_{65} &= mc_7 \sin \alpha, & A_{66} &= -\left(c_4 + \frac{1}{R(x)}\right) \sin \alpha, \\ A_{67} &= -\frac{m}{R(x)}, & A_{68} &= 0, & A_{69} &= -c_2 \sin \alpha, & A_{610} &= 0, \\ A_{71} &= mc_6 \sin \alpha, & A_{72} &= m^2 c_6 + \frac{fF_{44} \cos \alpha}{R(x)^2} - I_0 \omega^2, & A_{73} &= m \cos \alpha \left(c_6 + \frac{fF_{44}}{R(x)^2}\right), \\ A_{74} &= mc_7 \sin \alpha, & A_{75} &= m^2 c_7 - \frac{fF_{44} \cos \alpha}{R(x)^2} - I_1 \omega^2, & A_{76} &= -mc_4, \end{aligned}$$

$$\begin{aligned}
A_{77} &= -\frac{2 \sin \alpha}{R(x)}, \quad A_{78} = 0, \quad A_{79} = -mc_2, \quad A_{710} = 0, \\
A_{81} &= c_{13} \left( c_1 \sin \alpha + \frac{A_{11}}{R(x)^2} \cos \alpha + k_p c_2 \sin \alpha \right), \\
A_{82} &= mc_{13} \left( \frac{fF_{44}}{R^2} \cos \alpha + c_{11} + \frac{A_{11}}{R(x)^2} \cos \alpha + k_p c_2 \right), \\
A_{83} &= c_{13} \left( \frac{m^2 fF_{44}}{R(x)^2} + c_{11} \cos \alpha + k_p c_2 \cos \alpha - I_0 \omega^2 + k_w + \frac{m^2 k_p}{R(x)^2} \right), \\
A_{84} &= c_{13} \left( c_{12} \sin \alpha + \frac{B_{22}}{R(x)^2} \cos \alpha + k_p \frac{\sin \alpha}{R(x)} + k_p c_3 \sin \alpha \right), \\
A_{85} &= mc_{13} \left( -\frac{fF_{44}}{R(x)} + c_{12} + \frac{B_{22}}{R(x)^2} \cos \alpha + k_p c_3 \right), \\
A_{86} &= c_{13} \left( \frac{A_{12}}{R(x)} \frac{D_{11}}{c_1} \cos \alpha - \frac{B_{12}}{R(x)} \frac{B_{11}}{c_1} \cos \alpha - k_p \frac{B_{11}}{c_1} \right), \quad A_{87} = 0, \\
A_{88} &= -\frac{\sin \alpha}{R(x)}, \quad A_{89} = c_{13} \left( -\frac{A_{12}}{R(x)} \frac{B_{11}}{c_1} \cos \alpha + \frac{B_{12}}{R(x)} \frac{A_{11}}{c_1} \cos \alpha + k_p \frac{A_{11}}{c_1} \right), \quad A_{810} = 0, \\
A_{91} &= 2c_8 \sin^2 \alpha - I_1 \omega^2, \quad A_{92} = 2mc_8 \sin \alpha, \quad A_{93} = 2c_8 \sin \alpha \cos \alpha, \\
A_{94} &= 2c_9 \sin^2 \alpha - I_2 \omega^2, \quad A_{95} = 2mc_9 \sin \alpha, \quad A_{96} = -2c_5 \sin \alpha, \quad A_{97} = 0, \\
A_{98} &= 1, \quad A_{99} = -\left( c_3 + \frac{1}{R(x)} \right) 2 \sin \alpha, \quad A_{910} = -\frac{m}{R(x)}, \\
A_{101} &= mc_8 \sin \alpha, \quad A_{102} = m^2 c_8 - \frac{fF_{44} \cos \alpha}{R(x)} - I_1 \omega^2, \quad A_{103} = m \left( c_8 \cos \alpha - \frac{fF_{44}}{R(x)} \right), \\
A_{104} &= mc_9 \sin \alpha, \quad A_{105} = m^2 c_9 + fF_{44} - I_2 \omega^2, \quad A_{106} = -mc_5, \quad A_{107} = 0, \\
A_{108} &= 0, \quad A_{109} = -mc_3, \quad A_{1010} = -\frac{2 \sin \alpha}{R(x)}.
\end{aligned}$$